
AUTOMATO: AN OUT-OF-THE-BOX PERSISTENCE-BASED CLUSTERING ALGORITHM

Anonymous authors

Paper under double-blind review

ABSTRACT

We present AuToMATo, a novel clustering algorithm based on persistent homology. While AuToMATo is not parameter-free per se, we provide default choices for its parameters that make it into an out-of-the-box clustering algorithm that performs well across the board. AuToMATo combines the existing ToMATo clustering algorithm with a bootstrapping procedure in order to separate significant peaks of an estimated density function from non-significant ones. We perform a thorough comparison of AuToMATo (with its parameters fixed to their defaults) against many other state-of-the-art clustering algorithms. We find not only that AuToMATo compares favorably against parameter-free clustering algorithms, but in many instances also significantly outperforms even the best selection of parameters for other algorithms. AuToMATo is motivated by applications in topological data analysis, in particular the Mapper algorithm, where it is desirable to work with a clustering algorithm that does not need tuning of its parameters. Indeed, we provide evidence that AuToMATo performs well when used with Mapper. Finally, we provide an open-source implementation of AuToMATo in Python that is fully compatible with the standard *scikit-learn* architecture.

1 INTRODUCTION

Clustering techniques play a central role in understanding and interpreting data in a variety of fields. The idea is to divide a heterogeneous group of objects into groups based on a notion of similarity. This similarity is often measured with a distance or a metric on a data set. There exist many different clustering techniques (Anderberg, 1973; Duda et al., 2000), including hierarchical, centroid-based and density-based techniques, as well as techniques arising from probabilistic generative models. Each of these methods is proficient at finding clusters of a particular nature. Many of the most commonly used clustering algorithms require a selection of a parameters, a process which poses a considerable challenge when applying clustering to real-world problems.

In this work, we present and implement AuToMATo (*Automated Topological Mode Analysis Tool*), a novel clustering algorithm based on the topological clustering algorithm ToMATo (Chazal et al., 2013). The latter summarizes the prominences of peaks of a density function in a so-called persistence diagram. The user then selects a prominence threshold τ and retains all peaks whose prominence is above this threshold, which results in the final clustering. A simple heuristic to select τ is to sort the peaks by decreasing prominence, and to look for the largest gap between two consecutive prominence values (Chazal et al., 2013). While yielding reasonable results in general, this procedure is not very robust to small changes in the prominence values.

A more robust and sophisticated method is to perform a bottleneck bootstrap on the persistence diagram produced by ToMATo, which is precisely what AuToMATo does. That is, given a persistence diagram obtained by running ToMATo on a point cloud, AuToMATo produces a confidence region for that diagram with respect to the bottleneck distance, which translates into a choice of τ that determines the final clustering. While AuToMATo is not parameter-free per se, we provide default choices that make it perform well across the board. Unless stated otherwise, AuToMATo will henceforth refer to our algorithm with its parameters set to these defaults. We experimentally analyze the clustering performance of AuToMATo and we find that it not only outperforms parameter-free clustering algorithms, but often also even the best choice of hyperparameters for many parametric clustering algorithms. Parameter-free algorithms building on ToMATo exist in the literature, for ex-

ample, in Cotsakis et al. (2021) the final clustering is determined by fitting a curve to the values of prominence, and in Bois et al. (2024) significant values are separated from non-significant ones by adapting the process that produces the persistence diagrams. Indeed, the former algorithm is one of those that AuToMATo is shown to outperform.

We envision one important application of AuToMATo to be to the *Mapper* algorithm, introduced in Singh et al. (2007). Mapper constructs a graph that captures the topological structure of a data set. It relies on many parameters, one them being a clustering algorithm applied to various chunks of the data. Algorithms that depend heavily on a good choice of a tunable hyperparameter are generally not good candidates for usage with Mapper, as the best choice for the hyperparameter can vary significantly over the different chunks, and manually choosing a different hyperparameter for each may not be possible in practice. Thus, most choices of hyperparameter will generally perform badly on some of the subsets, leading to undesired results of Mapper. Thus AuToMATo can be seen as progress towards finding optimal parameters for Mapper, which is active area of research (Carrière et al., 2018; Chalapathi et al., 2021; Rosen et al., 2023). Running examples for Mapper with AuToMATo, we see that it is indeed a good choice for a clustering algorithm in this application when compared to parametric clustering algorithm such as DBSCAN.

2 BACKGROUND

2.1 PERSISTENCE AND THE TOMATO CLUSTERING ALGORITHM

Both ToMATo and AuToMATo rely on the theory of persistence (Edelsbrunner et al., 2002; Zomorodian & Carlsson, 2005; Carlsson, 2014) to quantify the prominence of peaks of (an estimate of) a density function, and to build a hierarchy of peaks. Given a topological space X equipped with a density function $f: X \rightarrow \mathbb{R}_{\geq 0}$, the first step of persistence is to build a filtration from X .

Definition 2.1. *Let X be a topological space and $f: X \rightarrow \mathbb{R}$ continuous. The **superlevelset filtration** of (X, f) is the family of superlevelsets $\{X_{\geq t} \mid t \in \mathbb{R}\}$, where $X_{\geq t} := f^{-1}([t, \infty))$.*

In the following we assume for ease of exposition that all local extrema of f have distinct values. The idea underlying ToMATo is to track the evolution of (the number of) connected components of $X_{\geq t}$ as t ranges from $+\infty$ to $-\infty$. In that process, the number of connected components of $X_{\geq t}$ remains constant, unless t passes through the value of a local extremum of f . As t passes through the value of a local maximum, a new connected component is “born” and added to the superlevelset $X_{\geq t}$. Similarly, as t passes through the value of a local minimum, two connected components of $X_{\geq t}$ are merged into one. ToMATo builds a hierarchy of local maxima of f by declaring that, as two components get merged, the component corresponding to the local maximum with higher value absorbs the other one and persists, whereas the component corresponding to the local maximum with lower value “dies”. Therefore, to each local maximum we associate a pair (b, d) where b denotes the birth and d the death time, respectively. The evolution of the connected components can be concisely recorded in a persistence diagram.

Definition 2.2. *Let $\{(b_l, d_l)\}_l$ denote the birth and death times of connected components of the superlevelset filtration $\{X_{\geq t}\}_{t \in \mathbb{R}}$ associated to the density $f: X \rightarrow \mathbb{R}$. The associated **persistence diagram**, denoted by $\text{Dgm}(X, f)$, is the multiset in the extended plane $\overline{\mathbb{R}^2} := \mathbb{R} \cup \{\pm\infty\}$ consisting of the points $\{(b_l, d_l)\}_l \subset \overline{\mathbb{R}^2}$ (counted with multiplicity) and the diagonal $\Delta := \{(x, x) \mid x \in \mathbb{R}\}$ (where each point on Δ has infinite multiplicity). For a given local maximum of f with birth time b_l and death time d_l , we refer to the difference $d_l - b_l$ as its **prominence** or **lifetime**.*

The reason for working in the extended plane is that, provided that f has a global maximum, the superlevelset filtration $X_{\geq t}$ will have a connected component that never dies, i.e., has death time equal to $-\infty$. See the red graph in Figure 1 for an illustration.

The persistence diagram $\text{Dgm}(X, f)$ provides a summary of f . The points of $\text{Dgm}(X, f)$ are in one-to-one correspondence with the local maxima of f , and twice the L^∞ -distance of a point to the diagonal Δ (i.e., its Euclidean vertical distance) equals its prominence.

We now outline how the ToMATo clustering algorithm works. Given a point cloud X ToMATo relies on the assumption that the points of X were sampled according to some unknown density function

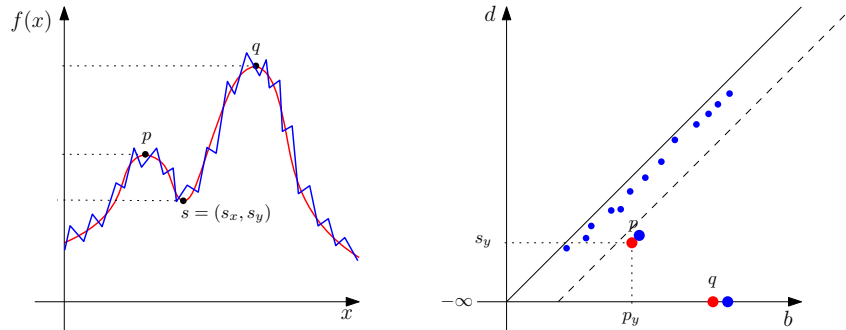
108 f . In a nutshell, ToMATo infers information about the local maxima of f by applying the above
 109 procedure to an estimate of f . ToMATo takes as input:

- 110 • **A neighborhood graph \mathcal{G} on the points of X .** Chazal et al. mostly use the δ -Rips graph
 111 and the k -nearest neighbor graph.¹
- 112 • **A density estimator \hat{f} .** Each vertex v of \mathcal{G} is assigned a non-negative value $\hat{f}(v)$ that corre-
 113 sponds to the estimated density at v . Chazal et al. propose two possible density estimators:
 114 the truncated Gaussian kernel density estimator and the distance-to-measure density, origi-
 115 nally introduced in Biau et al. (2011).²
- 116 • **A merging parameter $\tau \geq 0$.** This is a threshold that the prominence of a local maximum
 117 of the estimated density \hat{f} must clear for that local maximum to be deemed a feature.
 118

119 Given the inputs above, ToMATo proceeds as follows.

- 120 1. **Estimate the underlying density function \hat{f} at the points of X .**
- 121 2. **Apply a hill-climbing algorithm on \mathcal{G} .** Construct the neighborhood graph \mathcal{G} on the points
 122 of X , and construct a directed subgraph \mathcal{G}' of \mathcal{G} as follows: at each vertex v of \mathcal{G} , place
 123 a directed edge from v to its neighbor with highest value of \hat{f} , provided that that value is
 124 higher than $\hat{f}(v)$. If all neighbors of v have lower values, v is a peak of \hat{f} . This yields a
 125 collection of directed edges that form a spanning forest of the graph \mathcal{G} , consisting of one
 126 tree for each local maximum of \hat{f} . In particular, these trees yield a partition of the elements
 127 of X into pairwise disjoint sets that serves as a candidate clustering on X .
- 128 3. **Construct the persistence diagram.** Construct the persistence diagram $\text{Dgm}(\mathcal{G}, \hat{f})$ asso-
 129 ciated to the superlevelset filtration of $\hat{f}: \mathcal{G} \rightarrow \mathbb{R}$.
- 130 4. **Merge non-significant clusters.** Iteratively merge every cluster of prominence less than
 131 τ of the candidate clustering found in Step 2 into its parent cluster, i.e., into the cluster
 132 corresponding to the local maximum that it gets merged into in the superlevelset filtration
 133 of $\hat{f}: \mathcal{G} \rightarrow \mathbb{R}$. ToMATo outputs the resulting clustering of points of X , in which every
 134 cluster has prominence at least τ by construction.
 135

136 The reason why we can expect the persistence diagram of the approximated density to be “close”
 137 to the original one stems from the stability of persistence diagrams under the bottleneck distance
 138 (explained in Section 2.2). This is illustrated in Figure 1.



140
141
142
143
144
145
146
147
148
149
150
151 Figure 1: A function $f: K \rightarrow \mathbb{R}$, $K \subset \mathbb{R}$, in red, and an estimate \hat{f} of f in blue (left), with
 152 corresponding persistence diagrams $\text{Dgm}(K, f)$ and $\text{Dgm}(\mathcal{G}, \hat{f})$ consisting of the red and blue
 153 dots, respectively, together with a dashed line separating noise from features (right).
 154

155
156 ¹Given a point cloud, both of these undirected graphs have the set of data points as their vertex set. In the
 157 case of the δ -Rips graph, two vertices are connected iff they are at a distance of at most δ apart, whereas in the
 158 k -nearest neighbor graph, a data point is connected to another iff the latter is among the k -nearest neighbors of
 the first.

159 ²For a smoothing parameter $m \in (0, 1)$, and a given data point x , its empirical (unnormalized) distance-to-
 160 measure density is given by $\hat{f}(x) = \left(\frac{1}{k} \sum_{y \in N_k(x)} \|x - y\|^2 \right)^{-\frac{1}{2}}$, where $k = \lceil mn \rceil$, $N_k(x)$ denotes the set
 161 of the k nearest neighbors of x , and n is the cardinality of the data set.

In practice, the user must run ToMATo twice. First, ToMATo is run with $\tau = +\infty$ which is equivalent to computing the birth and death time of each local maximum of \hat{f} and hence the persistence diagram $\text{Dgm}(\mathcal{G}, \hat{f})$. From the diagram $\text{Dgm}(\mathcal{G}, \hat{f})$ the user then determines a merging parameter τ by visually identifying a large gap in $\text{Dgm}(\mathcal{G}, \hat{f})$ separating, say, C points corresponding to highly prominent peaks from the rest of the points. Then, ToMATo is run a second time with τ set to that value, which results in the final clustering of X into C clusters.

2.2 THE BOTTLENECK BOOTSTRAP

The bottleneck bootstrap, introduced in Chazal et al. (2017, Section 6), is used to separate significant features in persistence diagrams from non-significant ones. While it may be used in more general settings, we will restrict ourselves to the scenario of Section 2.1.

We first review the bottleneck distance, which is the standard distance measure between persistence diagrams (Edelsbrunner & Harer, 2010; Chazal et al., 2016).

Definition 2.3. Let Dgm_1 and Dgm_2 be two persistence diagrams that have finitely many points off the diagonal. Let π denote the set of bijections $\nu: \text{Dgm}_1 \rightarrow \text{Dgm}_2$. Given points $x = (x_1, x_2)$ and $y = (y_1, y_2)$ in $\overline{\mathbb{R}}^2$, let $\|x - y\|_\infty = \max\{|x_1 - y_1|, |x_2 - y_2|\}$ denote their L^∞ -distance, where we set $(+\infty) - (+\infty) = (-\infty) - (-\infty) = 0$. Then, the **bottleneck distance** between Dgm_1 and Dgm_2 is defined as

$$W_\infty(\text{Dgm}_1, \text{Dgm}_2) = \inf_{\nu \in \pi} \sup_{x \in \text{Dgm}_1} \|x - \nu(x)\|_\infty.$$

Note that a bijection $\nu: \text{Dgm}_1 \rightarrow \text{Dgm}_2$ is allowed to match an off-diagonal point of Dgm_1 to the diagonal of Dgm_2 , and vice versa.

We now outline the bottleneck bootstrap. Suppose that X is a sample consisting of n data points, drawn according to some unknown probability density function $f: K \rightarrow [0, 1]$, $K \subset \mathbb{R}^n$, and let $\mathcal{D} := \text{Dgm}(K, f)$ denote the corresponding (unknown) persistence diagram (we assume the density f and all of its estimates to be normalized here for ease of exposition). We estimate f and the connectivity of K with a density estimator and a neighborhood graph, respectively (as explained in Section 2.1). This allows us to compute $\hat{\mathcal{D}} := \text{Dgm}(X, \hat{f})$ (where \hat{f} is the estimate of f), which, in turn, serves as an estimate of \mathcal{D} .

Given a confidence level $\alpha \in (0, 1)$ and a number $B \in \mathbb{Z}_{\geq 1}$ of bootstrap iterations, the bottleneck bootstrap gives an estimate of q_α , which is defined by

$$\mathbb{P}(\sqrt{n}W_\infty(\mathcal{D}, \hat{\mathcal{D}}) \leq q_\alpha) = 1 - \alpha. \quad (1)$$

To that end, we first approximate f with the empirical measure P_n on X that assigns the probability mass of $1/n$ to each data point (note that this generally does not coincide with \hat{f}). This allows us to estimate the distribution

$$F(z) := \mathbb{P}(\sqrt{n}W_\infty(\mathcal{D}, \hat{\mathcal{D}}) \leq z)$$

with the distribution

$$\hat{F}(z) := \mathbb{P}(\sqrt{n}W_\infty(\hat{\mathcal{D}}^*, \hat{\mathcal{D}}) \leq z),$$

where $\hat{\mathcal{D}}^* := \text{Dgm}(X^*, \hat{f}^*)$ is the persistence diagram corresponding to a sample X^* of size n drawn from P_n , and the density \hat{f}^* and the connectivity of X^* are estimated using the same estimators as before. Note that X^* may be thought of as a sample drawn from X with replacement. The distribution \hat{F} itself is approximated by Monte Carlo as follows. We draw B samples X_1^*, \dots, X_B^* of size n from P_n , and for each of these B samples, we compute the persistence diagram $\hat{\mathcal{D}}_i^* := \text{Dgm}(X_i^*, \hat{f}_i^*)$ and the quantity $T_i^* := \sqrt{n}W_\infty(\hat{\mathcal{D}}_i^*, \hat{\mathcal{D}})$, $i = 1, \dots, B$. Finally, we use the function

$$\tilde{F}(z) := \frac{1}{B} \sum_{i=1}^B \mathbf{1}_{[0, z]}(T_i^*)$$

as an approximation of \hat{F} , and hence of F . Using this, we set

$$\hat{q}_\alpha := \inf\{z \mid \tilde{F}(z) \geq 1 - \alpha\}$$

to be our estimate of q_α . This estimate is asymptotically consistent if $\sup_z |\tilde{F}(z) - F(z)| \xrightarrow{f} 0$. If that is the case, it follows from Equation 1 that (asymptotically) the true, unknown persistence diagram \mathcal{D} is at bottleneck distance of at most \hat{q}_α/\sqrt{n} from $\hat{\mathcal{D}}$. Hence, points of $\hat{\mathcal{D}}$ that are at L^∞ -distance at most \hat{q}_α/\sqrt{n} from the diagonal could be matched to the diagonal under the bottleneck distance, and thus a point of $\hat{\mathcal{D}}$ is declared to be a significant feature iff it is at L^∞ -distance of at least \hat{q}_α/\sqrt{n} to the diagonal, i.e., iff its prominence is at least $2 \cdot \hat{q}_\alpha/\sqrt{n}$.

3 METHODOLOGY AND IMPLEMENTATION OF AUTOMATO

3.1 METHODOLOGY OF AUTOMATO

AuToMATo builds upon the ToMATo clustering scheme introduced in Chazal et al. (2013) and implemented in Glisse (2023). AuToMATo automates the step of visual inspection of the persistence diagram by means of the bottleneck bootstrap, thus promoting ToMATo to a clustering scheme that does not rely on human input.

More precisely, given a point cloud X to perform the clustering on, AuToMATo takes as input

- an instance of ToMATo with fixed neighborhood graph and density function estimators;
- a confidence level $\alpha \in (0, 1)$; and
- a number of bootstrap iterations $B \in \mathbb{Z}_{\geq 1}$.

Remark 3.1. *We point out that our implementation of AuToMATo comes with default values for each of the objects. Each of these values can, of course, be adjusted by the user. For details on these default values, see Subsection 3.2.*

In the present context the bottleneck bootstrap proceeds as follows. AuToMATo generates B bootstrap subsamples X_1^*, \dots, X_B^* of X , each of the same cardinality as X . Then, the underlying ToMATo instance with $\tau = +\infty$ and its neighborhood graph and density function estimators is used to compute the persistence diagram for X and each of X_1^*, \dots, X_B^* , yielding persistence diagrams $\hat{\mathcal{D}}$ and $\hat{\mathcal{D}}_1^*, \dots, \hat{\mathcal{D}}_B^*$, respectively. Using the bootstrapped diagrams $\hat{\mathcal{D}}_1^*, \dots, \hat{\mathcal{D}}_B^*$, a bottleneck bootstrap is performed on $\hat{\mathcal{D}}$. This yields a value \hat{q}_α that (asymptotically as $n \rightarrow \infty$) satisfies

$$\mathbb{P}(\sqrt{n}W_\infty(\mathcal{D}, \hat{\mathcal{D}}) \leq \hat{q}_\alpha) = 1 - \alpha,$$

where \mathcal{D} denotes the persistence diagram of the true, unknown density function from which X was sampled. Thus, points of $\hat{\mathcal{D}}$ of prominence at least $2 \cdot \hat{q}_\alpha/\sqrt{n}$ are declared to be significant features of $\hat{\mathcal{D}}$, and AuToMATo outputs its underlying ToMATo instance with prominence threshold set to $\tau = 2 \cdot \hat{q}_\alpha/\sqrt{n}$.

When computing the values $\sqrt{n}W_\infty(\hat{\mathcal{D}}_i^*, \hat{\mathcal{D}})$, $i = 1, \dots, B$, in the bottleneck bootstrap, we only consider points in $\hat{\mathcal{D}}_i^*$ and $\hat{\mathcal{D}}$ with finite lifetimes. The reason for this choice is that we consider peaks with infinite lifetime to be significant a priori. Moreover, some of the bootstrapped diagrams among the $\hat{\mathcal{D}}_1^*, \dots, \hat{\mathcal{D}}_B^*$ have a different number of points with infinite lifetime than the reference diagram $\hat{\mathcal{D}}$. In these cases, the bottleneck distance of the bootstrapped diagram to the reference diagram is infinite, which heavily distorts the distribution $\tilde{F}(z)$. This choice is justified by experiments.

3.2 IMPLEMENTATION OF AUTOMATO

We implemented AuToMATo in Python, and all of the code with documentation is available on GitHub.³ For a description of AuToMATo in pseudocode, see Algorithm 1. The algorithm has a worst-case complexity of $O(B(nd + n \log(n) + N^{1.5} \log N))$, where d is the dimensionality of the data and N is the maximal number of off-diagonal points across all relevant persistence diagram (which is generally much smaller than n); see Appendix A.2 for details. Note that the factor of B can be significantly decreased through parallelization.

While the input parameters may be adjusted by the user, the implementation provides default values whose choices we discuss presently.

³Anonymized GitHub-link

270
271
272
273
274
275
276
277
278
279
280
281
282
283
284
285
286
287
288
289
290
291
292
293
294
295
296
297
298
299
300
301
302
303
304
305
306
307
308
309
310
311
312
313
314
315
316
317
318
319
320
321
322
323

Algorithm 1: AuToMATo

Input: point cloud X of n data points; instance tom_τ of ToMATo with neighborhood graph and density function estimators, and prominence threshold τ ; confidence level $\alpha \in (0, 1)$; number of bootstrap iterations $B \in \mathbb{Z}_{\geq 1}$.

$\mathcal{D} \leftarrow \text{Dgm}(\text{tom}_\infty(X))$; // compute persistence diagram of point cloud

for $i = 1$ **to** B **do**

Let X_i^* be a subsample of X of size n , sampled with replacement;

$\mathcal{D}_i^* \leftarrow \text{Dgm}(\text{tom}_\infty(X_i^*))$; // compute persistence diagram of subsample

$d_i \leftarrow \sqrt{n}W_\infty^{\text{fin}}(\mathcal{D}_i^*, \mathcal{D})$; // compute bottleneck distance between finite points

end

Sort and reindex $\{\mathcal{D}_1^*, \dots, \mathcal{D}_B^*\}$ such that $d_1 \leq \dots \leq d_B$;

$k \leftarrow \lceil (1 - \alpha) \cdot B \rceil$;

$\hat{q}_\alpha \leftarrow d_k$;

$\tau \leftarrow 2 \cdot \hat{q}_\alpha / \sqrt{n}$;

Output: $\text{tom}_\tau(X)$; // copy of initial ToMATo instance with prominence threshold set to τ

Choice of ToMATo parameters: Our implementation of AuToMATo is such that the user can directly pass parameters to the underlying ToMATo instance. If no such arguments are provided AuToMATo uses the default choices for those parameters, as determined by the implementation of ToMATo given in Glisse (2023). In particular, AuToMATo uses the k -nearest neighbor graph and the (logarithm of the) distance-to-measure density estimators by default, each with $k = 10$. Of course, the persistence diagrams produced by ToMATo, and hence the output of AuToMATo, depend on this choice. This can lead to suboptimal clustering performance of AuToMATo; see Section 6.

Choice of α and B : By default, AuToMATo performs the bootstrap on $B = 1000$ subsamples of the input point cloud, and sets the confidence level to $\alpha = 0.35$. The choice of this latter parameter means that AuToMATo determines merely a 65% confidence region for the persistence diagram produced by the underlying ToMATo instance. While in bootstrapping the confidence level is often set to e.g. $\alpha = 0.05$, the seemingly strange choice of $\alpha = 0.35$ in the setting of AuToMATo is justified by experiments. The value of 65% seems to be low enough to offset some of the negative influence of using possibly non-optimized neighborhood graph and density estimators discussed in Section 6, while at the same time being high enough to yield good results when these estimators are chosen suitably. We point out that the value $\alpha = 0.35$ (as well as the value $B = 1000$) was decided on after running an early implementation of AuToMATo on just a few synthetic data sets. In particular, the choice was made *before* conducting the experiments in Section 4. AuToMATo is implemented in such a way that the parameter α can be adjusted *after* fitting and the clustering is automatically updated.

Our Python package for AuToMATo consists of two separate modules; one for AuToMATo itself, and one for the bottleneck bootstrap. Both are compatible with the *scikit-learn* architecture, and the latter may also be used as a stand-alone module for other scenarios. In addition to the functionality inherited from the *scikit-learn* API, the implementation of AuToMATo comes with options of

- adjusting the parameter α of a fitted instance of AuToMATo which automatically updates the resulting clustering without repeating the (computationally expensive) bootstrapping;
- plotting the persistence diagram and the prominence threshold found in the bootstrapping;
- setting a seed in order to make the creation of the bootstrap subsamples in AuToMATo deterministic, thus allowing for reproducible results; and
- parallelizing the bottleneck bootstrap for speed improvements.

Finally, our implementation of AuToMATo contains a parameter that allows the algorithm to label points as outliers. In a nutshell, a point is classified as an outlier if it is not among the nearest

neighbors of more than a specified percentage of its own nearest neighbors. This feature, however, is currently experimental (and is thus turned off by default).

4 EXPERIMENTS

4.1 CHOICE OF CLUSTERING ALGORITHMS FOR COMPARISON

We chose to compare AuToMATo with its default parameters against

- DBSCAN and its extension HDBSCAN;
- hierarchical clustering with Ward, single, complete and average linkage;
- the FINCH clustering algorithm (Sarfraz et al., 2019); and
- a clustering algorithm building on ToMATo stemming from the *Topology ToolKit* (TTK) suite (Tierny et al., 2018); in the following, we will refer to this as the *TTK-algorithm*.⁴

For DBSCAN, HDBSCAN and the hierarchical clustering algorithms mentioned above, we worked with their implementations in *scikit-learn*.⁵ For the FINCH clustering algorithm, we worked with the version available on GitHub.⁶ Indeed, we subclassed that version in order to make it compatible with the *scikit-learn* API. Similarly, we created a *scikit-learn* compatible version of the TTK-algorithm by combining code from TTK with the description of the algorithm given in Cotsakis et al. (2021, Section 5.2). While we included DBSCAN and HDBSCAN among the clustering algorithms to compare AuToMATo against because they are standard choices, we chose to include the hierarchical clustering algorithms because they are readily available through *scikit-learn*. Finally, we chose to include FINCH and the TTK-algorithm because, like AuToMATo, they are out-of-the-box (indeed, parameter-free) methods and are thus especially interesting to compare AuToMATo against.

4.2 CHOICE OF DATA SETS

The data sets on which we ran AuToMATo and the above clustering algorithms stem from the *Clustering Benchmarks* suite.⁷ We chose this collection as it comes with a large variety of different data sets, all of which are labeled by one or more ground truths, allowing for a fair and extensive comparison. The collection contains five recommended batteries of data sets from which we selected those (data set, ground truth)-pairs that we deemed reasonable for a general purpose parameter-free clustering algorithm. For instance, we chose to include the data set named `windows` that is part of the `wut`-battery, but not the data set named `windows` from the same battery (see Figure 5 in the appendix for an illustration). We chose to include the `windows` data set because AuToMATo determines clusters depending on connectivity, and topologically speaking, there is only one connected component in the `olympic` data set. Finally, we excluded all instances where the ground truth contains data points that are labeled as outliers, as outliers creation is currently an experimental feature in AuToMATo.

4.3 METHODOLOGY OF THE EXPERIMENTS

We min-max scaled each data set, fitted the clustering algorithms to them, and recorded the clustering performance of each result by computing the Fowlkes-Mallows score (Fowlkes & Mallows, 1983) of the clustering obtained and the respective ground truth. While the Fowlkes-Mallows score was originally defined for hierarchical clusterings only, it may be defined for general clusterings as follows. Given a clustering C found by an algorithm and a ground truth clustering G , one defines the Fowlkes-Mallows score as

$$\text{FMS} := \sqrt{\frac{\text{TP}}{\text{TP} + \text{FP}}} \cdot \sqrt{\frac{\text{TP}}{\text{TP} + \text{FN}}},$$

where

- TP is the number of pairs of data points which are in the same cluster in C and in G ;

⁴For the *Topology ToolKit*, see [topology-tool-kit.github.io/](https://github.com/TopologyToolKit/topology-tool-kit) (BSD license).

⁵scikit-learn.org/stable/modules/clustering.html

⁶github.com/ssarfraz/FINCH-Clustering (CC BY-NC-SA 4.0 license)

⁷clustering-benchmarks.gagolewski.com/ (CC BY-NC-ND 4.0 license)

378
379
380
381
382
383
384
385
386
387
388
389
390
391
392
393
394
395
396
397
398
399
400
401
402
403
404
405
406
407
408
409
410
411
412
413
414
415
416
417
418
419
420
421
422
423
424
425
426
427
428
429
430
431

- FP is the number of pairs of data points which are in the same cluster in G but not in C ; and
- FN is the number of pairs of data points which are not in the same cluster in G but are in the same cluster in C .

In other words, the Fowlkes-Mallows score is defined as the geometric mean of precision and recall of a classifier whose relevant elements are pairs of points that belong to the same cluster in both C and G . It may attain any value between 0 and 1, and these extremal values correspond to the worst and best possible clustering, respectively. We chose to use the Fowlkes-Mallows score as opposed to e.g. mutual information or any of the Rand indices, because the latter have been shown to exhibit biased behaviour depending on whether the clusters in the ground truth are mostly of similar sizes or not, see e.g. Romano et al. (2016); to the best of our knowledge, the Fowlkes-Mallows score does not suffer from such drawbacks. Moreover, we chose not to use any intrinsic measures of clustering performance since any such measure implicitly defines a further clustering algorithm to compare AuToMATo against, whereas we are interested in comparing AuToMATo against a predefined ground truth clustering.

We set the hyperparameters of the HDBSCAN, FINCH and the TTK-algorithm to their default values (as per their respective implementations). In contrast to this, we let the distance threshold parameter for the DBSCAN and the hierarchical clustering algorithms vary from 0.05 to 1.00 in increments of 0.05, with the goal of comparing AuToMATo against the best and worst performing version of these clustering algorithms. To account for the randomized component of AuToMATo, we ran it ten times, each time with a different seed.

While we restricted ourselves to instances where the ground truth does not contain any points labeled as outliers, some of the clustering algorithms in our list (DBSCAN and HDBSCAN) label some data points as outliers. In order to prevent these algorithms from getting systematically low Fowlkes-Mallows scores because of these outliers, we removed all the points labeled as outliers by these algorithms, and only computed the Fowlkes-Mallows score on the remaining points, both for these clustering algorithms and for AuToMATo. This of course gives an advantage to DBSCAN and HDBSCAN over AuToMATo.

In order to allow reproducibility, we chose a fixed seed for all our experiments, which can be found in our code on GitHub. We ran our experiments on a laptop with a 12th Gen Intel Core i7-1260P processor running at 2.10GHz.

4.4 RESULTS AND INTERPRETATION

Table 1 shows the average Fowlkes-Mallows score of each algorithm across all benchmarking data sets; for AuToMATo, it shows the average and the standard deviation across the ten runs. For those benchmarking data sets that come with more than one ground truth, we included only the best score of the respective algorithm. Similarly, we included only the best performing parameter selection for those algorithms that we ran with varying distance thresholds (which, of course, skews the comparison in favor of those algorithms). As Table 1 shows, AuToMATo outperforms each clustering algorithm on average across all data sets, thus showing that it is indeed a versatile and powerful out-of-the-box clustering algorithm. In particular, AuToMATo outperforms the TTK-algorithm, which also build on ToMATo.

Table 1: Average clustering performance of AuToMATo vs. reference clustering algorithms

Algorithm	Fowlkes-Mallows score
AuToMATo	0.8554±0.0228
DBSCAN	0.8457
Average linkage	0.8321
HDBSCAN	0.8209
Single linkage	0.8156
TTK clustering algorithm	0.8019
Complete linkage	0.7592

Continued on next page

Table 1: Average clustering performance of AuToMATo vs. reference clustering algorithms

Algorithm	Fowlkes-Mallows score
Ward linkage	0.5896
FINCH	0.5074

The scores of our experiments are reported in Tables 2 through 6 in Appendix A.3. As an illustration, Figure 2 shows that the best choice of parameter for DBSCAN sometimes outperforms AuToMATo, which is to be expected. However, on most data sets where this is the case, the results from AuToMATo are still competitive, and there is a significant number of instances where AuToMATo outperforms DBSCAN for all parameter selections, in some cases by a lot.

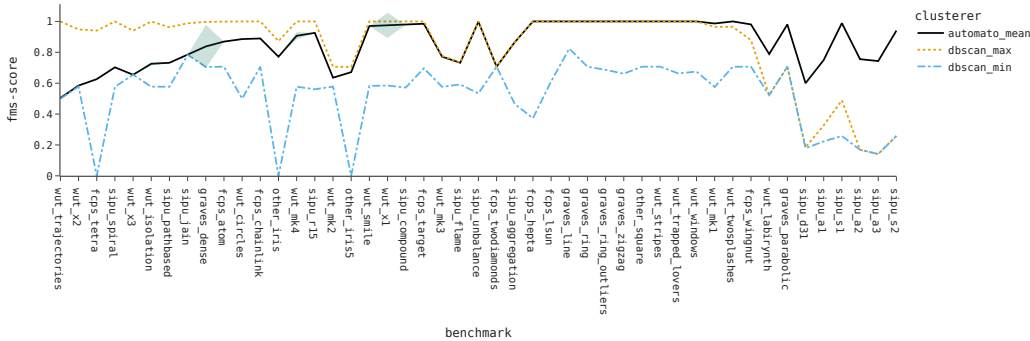


Figure 2: Fowlkes-Mallows score of AuToMATo and DBSCAN across benchmarking data sets. The shading of “automato_mean” indicates the standard deviation of the score across the ten runs.

5 APPLICATIONS OF AUTOMATO IN COMBINATION WITH MAPPER

The goal of *Mapper* (Singh et al., 2007) is to approximate the *Reeb graph* of a manifold M based on a sample from M . The input is a point cloud P with a filter function $P \rightarrow \mathbb{R}$, a collection of overlapping intervals $\mathcal{U} = \{U_1, \dots, U_n\}$ covering \mathbb{R} and a clustering algorithm. For each $U_i \in \mathcal{U}$, Mapper runs the clustering algorithm on the data points in the preimage $f^{-1}(U_i)$, creating a vertex for each cluster. Two vertices are then connected by an edge if the corresponding clusters (in different preimages) have some data points in common, yielding a graph that represents the shape of the data set. We ran the Mapper implementation of *giotto-tda* (Tausin et al., 2020) on a synthetic two-dimensional data set consisting of noisy samples from two concentric circles (see Figure 3a) with projection onto the x -axis as the filter function. We ran Mapper on the same interval cover with three different choices of clustering algorithms: AuToMATo, DBSCAN, and HDBSCAN. As can be seen in Figure 3b, using DBSCAN, we get many unwanted edges in the graph. HDBSCAN performs better, giving two cycles with some extra loops. The output of Mapper with AuToMATo is exactly the Reeb graph of two circles.

We further tested the combination of Mapper with AuToMATo on one of the standard applications of Mapper: the Miller-Reaven diabetes data set, where Mapper can be used detect two strains of diabetes that correspond to “flares” in the data set (see Singh et al. (2007, Section 5.1) for details).⁸ As can be seen in Figure 4, AuToMATo performs well in this task; the graphs show a central core of vertices corresponding to healthy patients, and two flares corresponding to the two strains of diabetes. We were not able to reproduce this using DBSCAN or HDBSCAN; Figure 4 shows the output of Mapper with these algorithms with their respective default parameters.

⁸The data set is available as part of the “locfit” R-package (Loader, 2024).

486
487
488
489
490
491
492
493
494
495
496
497
498
499
500
501
502
503
504
505
506
507
508
509
510
511
512
513
514
515
516
517
518
519
520
521
522
523
524
525
526
527
528
529
530
531
532
533
534
535
536
537
538
539

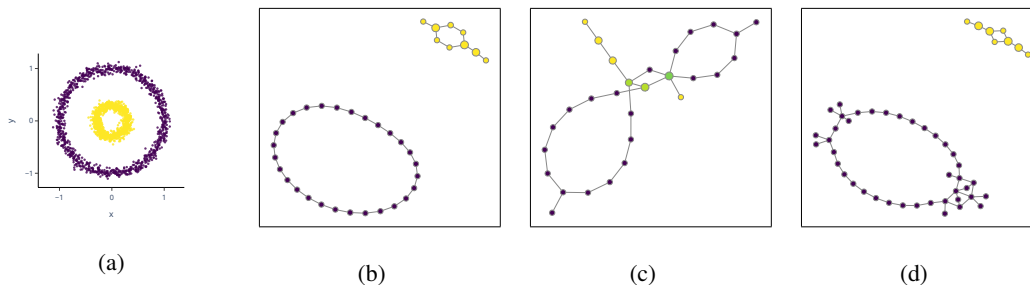


Figure 3: (a) input data set; result of Mapper with (b) AuToMATo; (c) DBSCAN; (d) HDBSCAN

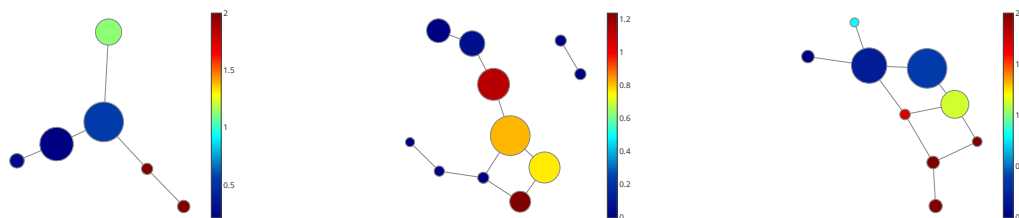


Figure 4: Mapper applied to the diabetes data set with AuToMATo (left); DBSCAN (center); HDBSCAN (right). Labels 0, 1 and 2 stand for “no”, “chemical” and “overt diabetes”.

6 DISCUSSION

We briefly outline some limitations of AuToMATo. AuToMATo comes with a choice of default values for its parameters. In particular, it resorts to the default values as implemented in ToMATo for the choice of neighborhood graph and density estimators. In ToMATo, the options for the neighborhood graph estimators are the δ -Rips graph and the k -nearest neighbor graph, relying on parameters $\delta > 0$ and $k \geq 1$, respectively; the options for the density estimators are the kernel density estimator and the distance-to-measure density estimator, which in turn rely parameters $h > 0$ and $m \in (0, 1)$, respectively (see the footnotes in Section 2.1 for their definitions). While for most data sets that we ran our experiments on these default estimators yielded good results, there are cases where adjusting them before running AuToMATo improves the clustering performance. Nevertheless, since finding a priori optimal parameters for the neighborhood graph and density estimators for a given data set is largely an open problem, we chose to stick to the default values for these estimators. Indeed, there are heuristics for the selection of the bandwidth in kernel density estimation (see Cotsakis et al. (2021, Section 4.1)) and the smoothing parameter in distance-to-measure density estimation (see Chazal et al. (2017, Section 7.1)), but these methods either lack theoretical justification, or would require running AuToMATo multiple times on the same data set with different parameters and selecting the best ones a posteriori, which undermines the intended use of AuToMATo as an out-of-the-box clustering algorithm.

Optimizing the choice of the neighborhood graph and density estimators is an aspect of AuToMATo that we plan to pursue in future work. Moreover, we plan to improve the currently experimental feature for outlier creation in AuToMATo discussed at the end of Section 3.2. Finally, it is natural to ask whether the results from Carrière et al. (2018) on optimal parameter selection in the Mapper algorithm can be adapted to the scenario where Mapper uses AuToMATo as its clustering algorithm.

REFERENCES

Michael R. Anderberg. Index. In *Cluster Analysis for Applications*, Probability and Mathematical Statistics: A Series of Monographs and Textbooks, pp. 355–359. Academic Press,

540 1973. doi: <https://doi.org/10.1016/B978-0-12-057650-0.50026-0>. URL <https://www.sciencedirect.com/science/article/pii/B9780120576500500260>.

541

542

543 Gérard Biau, Frédéric Chazal, David Cohen-Steiner, Luc Devroye, and Carlos Rodríguez. A

544 weighted k-nearest neighbor density estimate for geometric inference. *Electronic Journal of*

545 *Statistics*, 5(none):204 – 237, 2011. doi: 10.1214/11-EJS606. URL [https://doi.org/](https://doi.org/10.1214/11-EJS606)

546 [10.1214/11-EJS606](https://doi.org/10.1214/11-EJS606).

547 Alexandre Bois, Brian Tervil, and Laurent Oudre. Persistence-based clustering with outlier-

548 removing filtration. *Frontiers in Applied Mathematics and Statistics*, 10, 2024. doi: 10.3389/

549 [fams.2024.1260828](https://doi.org/10.3389/fams.2024.1260828).

550 Gunnar Carlsson. Topological pattern recognition for point cloud data. *Acta Numerica*, 23:289–368,

551 2014.

552

553 Mathieu Carrière, Bertrand Michel, and Steve Oudot. Statistical analysis and parameter selection

554 for mapper. *Journal of Machine Learning Research*, 19(12):1–39, 2018. URL [http://jmlr.](http://jmlr.org/papers/v19/17-291.html)

555 [org/papers/v19/17-291.html](http://jmlr.org/papers/v19/17-291.html).

556 Nithin Chalapathi, Youjia Zhou, and Bei Wang. Adaptive covers for mapper graphs using informa-

557 tion criteria. In *2021 IEEE International Conference on Big Data (Big Data)*, pp. 3789–3800,

558 2021. doi: 10.1109/BigData52589.2021.9671324.

559

560 Frédéric Chazal, Leonidas J Guibas, Steve Y Oudot, and Primoz Skraba. Persistence-based cluster-

561 ing in riemannian manifolds. *Journal of the ACM (JACM)*, 60(6):1–38, 2013.

562

563 Frédéric Chazal, Steve Y. Oudot, Marc Glisse, and Vin De Silva. *The Structure and Stability of*

564 *Persistence Modules*. SpringerBriefs in Mathematics. Springer Verlag, 2016. URL [https:](https://hal.inria.fr/hal-01330678)

565 [//hal.inria.fr/hal-01330678](https://hal.inria.fr/hal-01330678).

566 Frédéric Chazal, Brittany Fasy, Fabrizio Lecci, Bertrand Michel, Alessandro Rinaldo, and Larry A.

567 Wasserman. Robust topological inference: Distance to a measure and kernel distance. *J. Mach.*

568 *Learn. Res.*, 18:159:1–159:40, 2017. URL [http://jmlr.org/papers/v18/15-484.](http://jmlr.org/papers/v18/15-484.html)

569 [html](http://jmlr.org/papers/v18/15-484.html).

570 Ryan Cotsakis, Jim Shaw, Julien Tierny, and Joshua A. Levine. Implementing persistence-based

571 clustering of point clouds in the topology toolkit. In Ingrid Hotz, Talha Bin Masood, Filip Sadlo,

572 and Julien Tierny (eds.), *Topological Methods in Data Analysis and Visualization VI*, pp. 343–357,

573 Cham, 2021. Springer International Publishing. ISBN 978-3-030-83500-2.

574

575 Richard O. Duda, Peter E. Hart, and David G. Stork. *Pattern Classification (2nd Edition)*. Wiley-

576 Interscience, USA, 2000. ISBN 0471056693.

577 Edelsbrunner, Letscher, and Zomorodian. Topological persistence and simplification. *Discrete*

578 *& Computational Geometry*, 28(4):511–533, Nov 2002. ISSN 1432-0444. doi: 10.1007/

579 [s00454-002-2885-2](https://doi.org/10.1007/s00454-002-2885-2). URL <https://doi.org/10.1007/s00454-002-2885-2>.

580 H. Edelsbrunner and J. Harer. *Computational Topology: An Introduction*. Applied Mathemat-

581 ics. American Mathematical Society, 2010. ISBN 9780821849255. URL [https://books.](https://books.google.fr/books?id=MDXa6gFRZuIC)

582 [google.fr/books?id=MDXa6gFRZuIC](https://books.google.fr/books?id=MDXa6gFRZuIC).

583

584 A. Efrat, A. Itai, and M. J. Katz. Geometry helps in bottleneck matching and related problems.

585 *Algorithmica*, 31(1):1–28, Sep 2001. ISSN 1432-0541. doi: 10.1007/s00453-001-0016-8. URL

586 <https://doi.org/10.1007/s00453-001-0016-8>.

587 Edward B Fowlkes and Colin L Mallows. A method for comparing two hierarchical clusterings.

588 *Journal of the American statistical association*, 78(383):553–569, 1983.

589

590 Marc Glisse. persistence-based clustering. In *GUDHI User and Reference Manual*. GUDHI Ed-

591 itorial Board, 3.9.0 edition, 2023. URL [https://gudhi.inria.fr/python/3.9.0/](https://gudhi.inria.fr/python/3.9.0/clustering.html)

592 [clustering.html](https://gudhi.inria.fr/python/3.9.0/clustering.html). Available under MIT license.

593 Catherine Loader. *locfit: Local Regression, Likelihood and Density Estimation*, 2024. URL [https:](https://CRAN.R-project.org/package=locfit)

[//CRAN.R-project.org/package=locfit](https://CRAN.R-project.org/package=locfit). R package version 1.5-9.9.

594 Simone Romano, Xuan Vinh Nguyen, James Bailey, and Karin Verspoor. Adjusting for chance
595 clustering comparison measures. *J. Mach. Learn. Res.*, 17:134:1–134:32, 2016. URL <https://jmlr.org/papers/v17/15-627.html>.
596
597

598 P. Rosen, M. Hajij, and B. Wang. Homology-preserving multi-scale graph skeletonization using
599 mapper on graphs. In *2023 Topological Data Analysis and Visualization (TopoInVis)*,
600 pp. 10–20, Los Alamitos, CA, USA, oct 2023. IEEE Computer Society. doi: 10.1109/
601 TopoInVis60193.2023.00008. URL <https://doi.ieeecomputersociety.org/10.1109/TopoInVis60193.2023.00008>.
602

603 M. Saquib Sarfraz, Vivek Sharma, and Rainer Stiefelhagen. Efficient parameter-free clustering using
604 first neighbor relations. In *Proceedings of the IEEE Conference on Computer Vision and Pattern
605 Recognition (CVPR)*, pp. 8934–8943, 2019.

606 Gurjeet Singh, Facundo Mémoli, Gunnar E Carlsson, et al. Topological methods for the analysis of
607 high dimensional data sets and 3d object recognition. *PBG@ Eurographics*, 2:091–100, 2007.
608

609 Guillaume Tauzin, Umberto Lupo, Lewis Tunstall, Julian Burella Pérez, Matteo Caorsi, Anibal
610 Medina-Mardones, Alberto Dassatti, and Kathryn Hess. giotto-tda: A topological data analysis
611 toolkit for machine learning and data exploration, 2020.

612 Julien Tierny, Guillaume Favelier, Joshua A. Levine, Charles Gueunet, and Michael Michaux. The
613 topology toolkit. *IEEE Transactions on Visualization and Computer Graphics*, 24(1):832–842,
614 January 2018. ISSN 1077-2626. doi: 10.1109/TVCG.2017.2743938. Funding Information:
615 This work is partially supported by the Bpifrance grant “AVIDO” (Programme d’Investissements
616 d’Avenir FSN2, reference P112017-2661376/DOS0021427) and by the National Science Founda-
617 tion IIS-1654221. We would like to thank the reviewers for their thoughtful remarks and sug-
618 gestions. We would also like to thank Attila Gyulassy, Julien Jomier and Joachim Pouderoux for
619 insightful discussions and Will Schroeder, who encouraged us to write this manuscript. Publisher
620 Copyright: © 1995-2012 IEEE.

621 Afra Zomorodian and Gunnar Carlsson. Computing persistent homology. *Discrete & Computational
622 Geometry*, 33(2):249–274, Feb 2005. ISSN 1432-0444. doi: 10.1007/s00454-004-1146-y. URL
623 <https://doi.org/10.1007/s00454-004-1146-y>.
624
625
626
627
628
629
630
631
632
633
634
635
636
637
638
639
640
641
642
643
644
645
646
647

A APPENDIX

A.1 ABOUT THE CHOICE OF DATA SETS

As explained in Section 4.2, we chose to include the data set named `windows` from the battery named `wut`, but not the data set named `olympic` from the same battery. Those are illustrated in Figure 5. In that figure, the data points are colored according to the ground truth clustering.

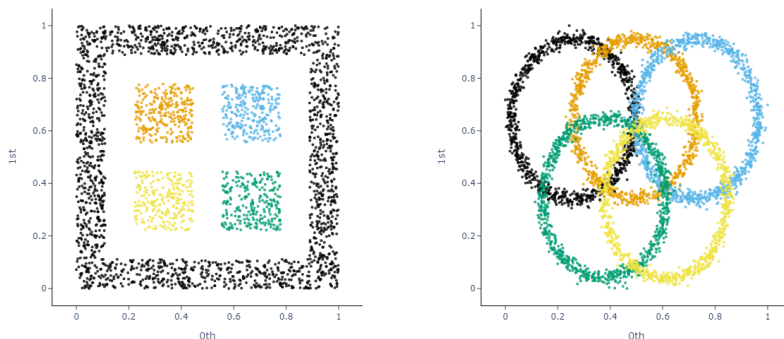


Figure 5: The data sets named `windows` (left) and `olympic` (right) from the `wut`-battery.

A.2 COMPLEXITY ANALYSIS OF ALGORITHM 1

Recall from Chazal et al. (2013, Section 2) that, if an estimated density and a neighborhood graph are provided, ToMATo has a worst-case time complexity in $O(n \log(n) + m\alpha(n))$, where n and m are the number of vertices and edges of the neighborhood graph, respectively, and α denotes the inverse Ackermann function (note that n equals the number of data points). By default, ToMATo (and hence AuToMATo) works with the k -nearest neighbor graph and distance-to-measure density estimators, where the latter relies itself on the k -nearest neighbor graph (each with $k = 10$). Taking into account the known complexity bound $O(nd)$ for the creation of the k -nearest neighbor graph (where d is the dimensionality of the data), and using the fact that $m \in O(n)$ for this graph, this leads to a worst-case time complexity in $O(nd + n \log(n))$ for a single run of ToMATo. Creating the bootstrap samples X_i^* , $i = 1, \dots, B$, has complexity in $O(Bn)$; computing the values $\sqrt{n}W_\infty^{\text{fin}}(\mathcal{D}_i^*, \mathcal{D})$, $i = 1, \dots, B$, has worst-case complexity $O(BN^{1.5} \log(N))$ (see e.g. Efrat et al. (2001); here N denotes the maximal number of off-diagonal points across all relevant persistence diagram), and sorting them has worst case complexity in $O(B \log(B))$. Combined, this leads to a worst-case complexity for AuToMATo in $O(B(nd + n \log(n) + N^{1.5} \log(N)) + B \log(B))$. Using that B is a constant, we obtain the runtime claimed in the main body.

A.3 BENCHMARKING RESULTS

In this subsection we report the Fowlkes-Mallows scores coming from comparing AuToMATo to the other clustering algorithms, as explained in Section 4. For those benchmarking data sets that come with more than one ground truth, we report the scores for each of those, and different ground truths are indicated by the last digit in the data set name. Moreover, each table is sorted according to increasing difference in clustering performance of AuToMATo and the respective clustering algorithm that AuToMATo is being compared against. As is customary, we indicate the score stemming from the best performing clustering algorithm in bold. Finally, each of the table is accompanied by a graph similar to the one depicted in Figure 2. Note that, in particular, that those figures indicate only the score corresponding to the ground truth on which the respective clustering algorithm performs best on.

Table 2: Fowlkes-Mallows scores of AuToMATo vs. DBSCAN

Dataset	automato_mean	dbscan_max	dbscan_min
sipu_r15_2	0.4867±0.0000	1.0000	0.5607
wut_trajectories_0	0.5038±0.0107	1.0000	0.4999
wut_x3_0	0.5153±0.0000	0.9398	0.5149
wut_x2_0	0.5846±0.0000	0.9483	0.5779
sipu_r15_1	0.5436±0.0000	0.8954	0.5021
fcps_tetra_0	0.6261±0.0000	0.9403	0.0000
sipu_pathbased_0	0.6517±0.0000	0.9569	0.5769
sipu_spiral_0	0.7028±0.0000	1.0000	0.5756
wut_isolation_0	0.7256±0.0113	1.0000	0.5773
sipu_pathbased_1	0.7322±0.0000	0.9620	0.5170
sipu_jain_0	0.7837±0.0000	0.9880	0.7837
graves_dense_0	0.8377±0.1396	0.9970	0.7053
sipu_compound_0	0.8616±0.0000	1.0000	0.4972
fcps_atom_0	0.8694±0.0000	1.0000	0.7067
wut_circles_0	0.8857±0.0000	1.0000	0.4998
fcps_chainlink_0	0.8896±0.0000	1.0000	0.7068
other_iris_0	0.7715±0.0000	0.8721	0.0000
wut_mk4_0	0.9072±0.0234	1.0000	0.5770
wut_mk2_0	0.6356±0.0000	0.7068	0.5778
sipu_compound_4	0.9442±0.0000	1.0000	0.5523
wut_x3_1	0.6546±0.0000	0.7042	0.6546
graves_zigzag_1	0.6720±0.0000	0.7149	0.4446
other_iris5_0	0.6712±0.0000	0.7046	0.0000
wut_smile_1	0.9701±0.0000	1.0000	0.5825
wut_x1_0	0.9741±0.0818	1.0000	0.5846
fcps_target_0	0.9850±0.0000	1.0000	0.6963
wut_smile_0	0.9681±0.0000	0.9753	0.5471
wut_mk3_0	0.7720±0.0000	0.7774	0.5764
sipu_compound_1	0.9786±0.0000	0.9825	0.5715
sipu_flame_0	0.7320±0.0000	0.7341	0.5918
sipu_unbalance_0	0.9986±0.0008	1.0000	0.5339
fcps_twodiamonds_0	0.7067±0.0000	0.7067	0.7067
sipu_aggregation_0	0.8652±0.0000	0.8652	0.4653
wut_stripes_0	1.0000±0.0000	1.0000	0.7070
wut_trapped_lovers_0	1.0000±0.0000	1.0000	0.6632
wut_windows_0	1.0000±0.0000	1.0000	0.6753
fcps_hepta_0	1.0000±0.0000	1.0000	0.3727
fcps_lsun_0	1.0000±0.0000	1.0000	0.6111
graves_line_0	1.0000±0.0000	1.0000	0.8238
graves_ring_0	1.0000±0.0000	1.0000	0.7068
graves_ring_outliers_0	1.0000±0.0000	1.0000	0.6863
graves_zigzag_0	1.0000±0.0000	1.0000	0.5328
other_square_0	1.0000±0.0000	1.0000	0.7068
wut_mk1_0	0.9866±0.0000	0.9651	0.5754
wut_twosplashes_0	1.0000±0.0000	0.9649	0.7062
fcps_wingnut_0	0.9805±0.0000	0.8784	0.7068
graves_parabolic_1	0.6916±0.0000	0.5000	0.4999
wut_labyrinth_0	0.7884±0.0000	0.5221	0.5221
graves_parabolic_0	0.9802±0.0000	0.7068	0.7068
sipu_d31_0	0.6001±0.0085	0.1846	0.1787
sipu_a1_0	0.7499±0.0000	0.3269	0.2229
sipu_r15_0	0.9258±0.0000	0.4551	0.2552
sipu_s1_0	0.9888±0.0000	0.4890	0.2581

Continued on next page

Table 2: Fowlkes-Mallows scores of AuToMATo vs. DBSCAN

Dataset	automato_mean	dbscan_max	dbscan_min
sipu_a2_0	0.7555±0.0000	0.1685	0.1685
sipu_a3_0	0.7434±0.0000	0.1410	0.1410
sipu_s2_0	0.9405±0.0000	0.2581	0.2581

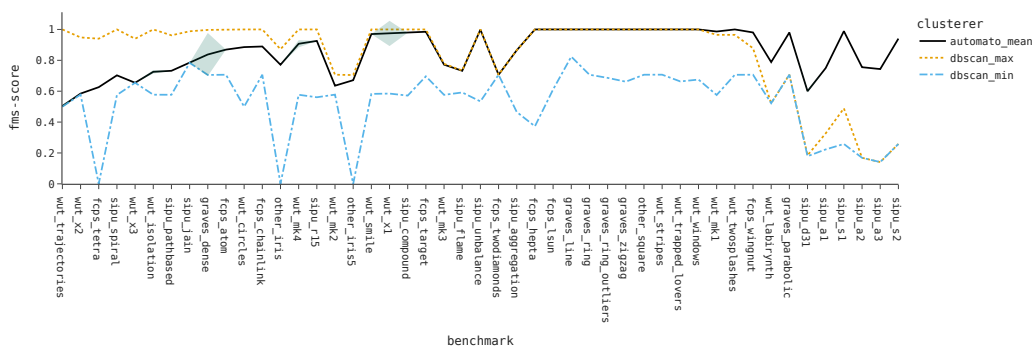


Figure 6: Comparison of AuToMATo and DBSCAN.

Table 3: Fowlkes-Mallows scores of AuToMATo vs. hierarchical clustering with average linkage

Dataset	automato_mean	linkage_average_max	linkage_average_min
sipu_r15_2	0.4867±0.0000	1.0000	0.3971
wut_trajectories_0	0.5038±0.0107	1.0000	0.3115
fcps_tetra_0	0.6261±0.0000	1.0000	0.0651
sipu_r15_1	0.5436±0.0000	0.8954	0.4435
sipu_d31_0	0.6001±0.0085	0.9322	0.1787
wut_x3_0	0.5153±0.0000	0.8389	0.3343
wut_x3_1	0.6546±0.0000	0.9747	0.2693
fcps_twodiamonds_0	0.7067±0.0000	0.9925	0.1287
sipu_a2_0	0.7555±0.0000	0.9432	0.1685
sipu_a1_0	0.7499±0.0000	0.9268	0.2229
sipu_a3_0	0.7434±0.0000	0.8825	0.1410
sipu_aggregation_0	0.8652±0.0000	0.9932	0.1785
sipu_pathbased_1	0.7322±0.0000	0.8564	0.2058
graves_dense_0	0.8377±0.1396	0.9604	0.6633
sipu_pathbased_0	0.6517±0.0000	0.7704	0.1848
wut_x2_0	0.5846±0.0000	0.7001	0.2782
wut_circles_0	0.8857±0.0000	1.0000	0.2369
wut_mk3_0	0.7720±0.0000	0.8771	0.0876
wut_mk2_0	0.6356±0.0000	0.7068	0.1421
sipu_r15_0	0.9258±0.0000	0.9900	0.2552
graves_zigzag_1	0.6720±0.0000	0.7202	0.4380
other_iris_0	0.7715±0.0000	0.8080	0.0791
other_iris5_0	0.6712±0.0000	0.7042	0.0451
wut_x1_0	0.9741±0.0818	1.0000	0.3070
sipu_jain_0	0.7837±0.0000	0.7904	0.1736
wut_mk1_0	0.9866±0.0000	0.9933	0.2037
sipu_unbalance_0	0.9986±0.0008	0.9995	0.5339
fcps_hepta_0	1.0000±0.0000	1.0000	0.3727

Continued on next page

810
811
812
813
814
815
816
817
818
819
820
821
822
823
824
825
826
827
828
829
830
831
832
833
834
835
836
837
838
839
840
841
842
843
844
845
846
847
848
849
850
851
852
853
854
855
856
857
858
859
860
861
862
863

Table 3: Fowlkes-Mallows scores of AuToMATo vs. hierarchical clustering with average linkage

Dataset	automato_mean	linkage_average_max	linkage_average_min
sipu_flame_0	0.7320±0.0000	0.7320	0.0913
sipu_s1_0	0.9888±0.0000	0.9821	0.2581
sipu_compound_0	0.8616±0.0000	0.8431	0.2207
sipu_compound_4	0.9442±0.0000	0.9224	0.1985
sipu_compound_1	0.9786±0.0000	0.9546	0.1922
sipu_s2_0	0.9405±0.0000	0.9097	0.2581
wut_smile_1	0.9701±0.0000	0.8726	0.4041
fcps_atom_0	0.8694±0.0000	0.7491	0.2555
graves_parabolic_1	0.6916±0.0000	0.5708	0.2135
sipu_spiral_0	0.7028±0.0000	0.5756	0.1919
wut_mk4_0	0.9072±0.0234	0.7714	0.2071
wut_smile_0	0.9681±0.0000	0.8221	0.4303
wut_isolation_0	0.7256±0.0113	0.5773	0.1651
graves_line_0	1.0000±0.0000	0.8238	0.3047
fcps_chainlink_0	0.8896±0.0000	0.7068	0.1456
fcps_target_0	0.9850±0.0000	0.7986	0.3285
fcps_wingnut_0	0.9805±0.0000	0.7739	0.1101
fcps_lsun_0	1.0000±0.0000	0.7896	0.1735
graves_ring_0	1.0000±0.0000	0.7780	0.2638
graves_parabolic_0	0.9802±0.0000	0.7580	0.1598
graves_ring_outliers_0	1.0000±0.0000	0.7767	0.2801
other_square_0	1.0000±0.0000	0.7413	0.1746
wut_labirynth_0	0.7884±0.0000	0.5221	0.2306
wut_stripes_0	1.0000±0.0000	0.7070	0.1082
wut_twosplashes_0	1.0000±0.0000	0.7062	0.4837
wut_windows_0	1.0000±0.0000	0.6753	0.1194
wut_trapped_lovers_0	1.0000±0.0000	0.6632	0.1077
graves_zigzag_0	1.0000±0.0000	0.6616	0.3008

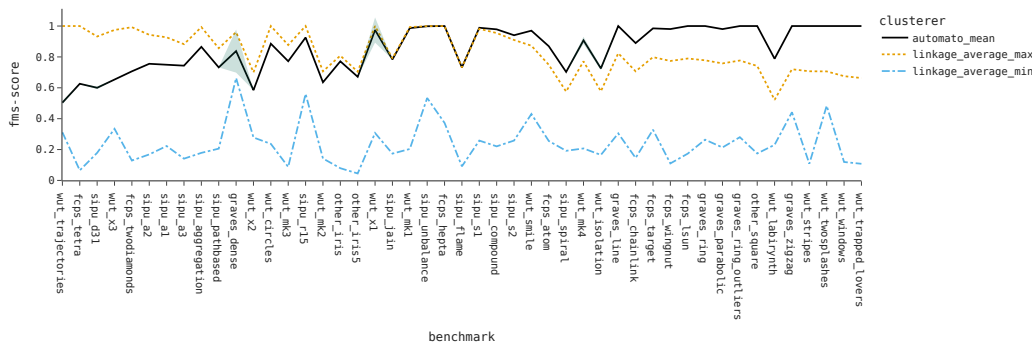


Figure 7: Comparison of AuToMATo and agglomerative clustering with average linkage.

Table 4: Fowlkes-Mallows scores of AuToMATo vs. HDBSCAN

Dataset	automato_mean	automato_std	hdbscan
wut_trajectories_0	0.5038±0.0107	0.0107	1.0000
wut_x3_0	0.5153±0.0000	0.0000	0.8959
wut_x2_0	0.5846±0.0000	0.0000	0.9344

Continued on next page

Table 4: Fowlkes-Mallows scores of AuToMATo vs. HDBSCAN

Dataset	automato_mean	automato_std	hdbscan
864 sipu_spiral_0	0.7028±0.0000	0.0000	0.9815
865 sipu_flame_0	0.7320±0.0000	0.0000	0.9900
866 sipu_d31_0	0.6001±0.0085	0.0085	0.8231
867 sipu_jain_0	0.7837±0.0000	0.0000	0.9779
871 fcps_tetra_0	0.6261±0.0000	0.0000	0.8157
872 graves_dense_0	0.8377±0.1396	0.1396	0.9894
873 sipu_pathbased_1	0.7322±0.0000	0.0000	0.8634
874 fcps_atom_0	0.8694±0.0000	0.0000	1.0000
875 sipu_pathbased_0	0.6517±0.0000	0.0000	0.7815
876 fcps_chainlink_0	0.8896±0.0000	0.0000	1.0000
877 sipu_r15_0	0.9258±0.0000	0.0000	0.9932
878 sipu_a1_0	0.7499±0.0000	0.0000	0.8081
879 wut_x3_1	0.6546±0.0000	0.0000	0.6972
880 other_iris5_0	0.6712±0.0000	0.0000	0.7042
881 wut_x1_0	0.9741±0.0818	0.0818	1.0000
882 sipu_compound_1	0.9786±0.0000	0.0000	1.0000
883 sipu_compound_4	0.9442±0.0000	0.0000	0.9656
884 fcps_target_0	0.9850±0.0000	0.0000	1.0000
885 sipu_compound_0	0.8616±0.0000	0.0000	0.8751
886 sipu_unbalance_0	0.9986±0.0008	0.0008	1.0000
887 graves_zigzag_1	0.6720±0.0000	0.0000	0.6720
888 sipu_aggregation_0	0.8652±0.0000	0.0000	0.8652
889 wut_stripes_0	1.0000±0.0000	0.0000	1.0000
890 wut_trapped_lovers_0	1.0000±0.0000	0.0000	1.0000
891 wut_windows_0	1.0000±0.0000	0.0000	1.0000
892 fcps_hepta_0	1.0000±0.0000	0.0000	1.0000
893 fcps_lsun_0	1.0000±0.0000	0.0000	1.0000
894 graves_line_0	1.0000±0.0000	0.0000	1.0000
895 graves_ring_0	1.0000±0.0000	0.0000	1.0000
896 graves_ring_outliers_0	1.0000±0.0000	0.0000	1.0000
897 graves_zigzag_0	1.0000±0.0000	0.0000	1.0000
898 other_square_0	1.0000±0.0000	0.0000	1.0000
899 other_iris_0	0.7715±0.0000	0.0000	0.7715
900 wut_mk3_0	0.7720±0.0000	0.0000	0.7719
901 wut_mk1_0	0.9866±0.0000	0.0000	0.9863
902 sipu_a3_0	0.7434±0.0000	0.0000	0.7415
903 sipu_a2_0	0.7555±0.0000	0.0000	0.7502
904 sipu_r15_2	0.4867±0.0000	0.0000	0.4671
905 sipu_r15_1	0.5436±0.0000	0.0000	0.5212
906 wut_isolation_0	0.7256±0.0113	0.0113	0.6377
907 fcps_wingnut_0	0.9805±0.0000	0.0000	0.8725
908 sipu_s1_0	0.9888±0.0000	0.0000	0.8717
909 sipu_s2_0	0.9405±0.0000	0.0000	0.7410
910 wut_mk4_0	0.9072±0.0234	0.0234	0.6459
911 wut_labrynth_0	0.7884±0.0000	0.0000	0.5134
912 graves_parabolic_1	0.6916±0.0000	0.0000	0.3616
913 fcps_twodiamonds_0	0.7067±0.0000	0.0000	0.2886
914 wut_mk2_0	0.6356±0.0000	0.0000	0.1574
915 wut_smile_0	0.9681±0.0000	0.0000	0.4000
916 wut_smile_1	0.9701±0.0000	0.0000	0.3714
917 graves_parabolic_0	0.9802±0.0000	0.0000	0.3526
wut_twosplashes_0	1.0000±0.0000	0.0000	0.3074
wut_circles_0	0.8857±0.0000	0.0000	0.1204

918
919
920
921
922
923
924
925
926
927
928
929
930
931
932
933
934
935
936
937
938
939
940
941
942
943
944
945
946
947
948
949
950
951
952
953
954
955
956
957
958
959
960
961
962
963
964
965
966
967
968
969
970
971

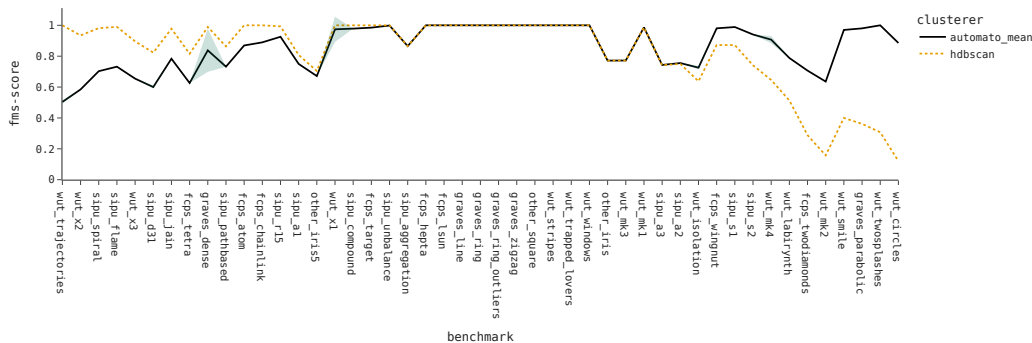


Figure 8: Comparison of AuToMATo and HDBSCAN.

Table 5: Fowlkes-Mallows scores of AuToMATo vs. hierarchical clustering with single linkage

Dataset	automato_mean	linkage_single_max	linkage_single_min
sipu_r15_2	0.4867±0.0000	1.0000	0.5607
wut_trajectories_0	0.5038±0.0107	1.0000	0.4999
sipu_r15_1	0.5436±0.0000	0.8954	0.5021
fcps_tetra_0	0.6261±0.0000	0.9296	0.0829
sipu_spiral_0	0.7028±0.0000	1.0000	0.5756
wut_isolation_0	0.7256±0.0113	1.0000	0.5773
wut_x3_0	0.5153±0.0000	0.7347	0.4951
sipu_jain_0	0.7837±0.0000	0.9510	0.7837
fcps_atom_0	0.8694±0.0000	1.0000	0.7067
wut_circles_0	0.8857±0.0000	1.0000	0.4998
fcps_chainlink_0	0.8896±0.0000	1.0000	0.7068
wut_mk4_0	0.9072±0.0234	1.0000	0.5770
sipu_compound_0	0.8616±0.0000	0.9454	0.4972
sipu_pathbased_0	0.6517±0.0000	0.7337	0.5769
sipu_pathbased_1	0.7322±0.0000	0.8091	0.5170
graves_dense_0	0.8377±0.1396	0.9096	0.6882
wut_mk2_0	0.6356±0.0000	0.7068	0.6007
graves_zigzag_1	0.6720±0.0000	0.7344	0.4446
wut_x2_0	0.5846±0.0000	0.6437	0.5105
other_iris5_0	0.6712±0.0000	0.7042	0.0451
wut_smile_1	0.9701±0.0000	1.0000	0.5825
wut_x1_0	0.9741±0.0818	0.9920	0.5846
fcps_target_0	0.9850±0.0000	1.0000	0.6963
wut_smile_0	0.9681±0.0000	0.9748	0.5471
sipu_unbalance_0	0.9986±0.0008	1.0000	0.5339
fcps_twodiamonds_0	0.7067±0.0000	0.7067	0.7067
wut_x3_1	0.6546±0.0000	0.6546	0.6140
sipu_aggregation_0	0.8652±0.0000	0.8652	0.4653
wut_stripes_0	1.0000±0.0000	1.0000	0.7070
wut_trapped_lovers_0	1.0000±0.0000	1.0000	0.6632
wut_windows_0	1.0000±0.0000	1.0000	0.6753
fcps_hepta_0	1.0000±0.0000	1.0000	0.3727
graves_line_0	1.0000±0.0000	1.0000	0.8238
graves_ring_0	1.0000±0.0000	1.0000	0.7068
graves_ring_outliers_0	1.0000±0.0000	1.0000	0.6863
graves_zigzag_0	1.0000±0.0000	1.0000	0.5381

Continued on next page

Table 5: Fowlkes-Mallows scores of AuToMATo vs. hierarchical clustering with single linkage

Dataset	automato_mean	linkage_single_max	linkage_single_min
sipu_flame_0	0.7320±0.0000	0.7320	0.4598
other_iris_0	0.7715±0.0000	0.7715	0.1223
other_square_0	1.0000±0.0000	0.9990	0.7068
fcps_lsun_0	1.0000±0.0000	0.9983	0.6111
wut_twosplashes_0	1.0000±0.0000	0.9850	0.7062
sipu_compound_1	0.9786±0.0000	0.9180	0.5715
sipu_compound_4	0.9442±0.0000	0.8824	0.5523
wut_mk1_0	0.9866±0.0000	0.8866	0.5754
fcps_wingnut_0	0.9805±0.0000	0.8087	0.7068
graves_parabolic_1	0.6916±0.0000	0.5000	0.4979
wut_mk3_0	0.7720±0.0000	0.5764	0.5314
wut_labirynth_0	0.7884±0.0000	0.5221	0.5221
graves_parabolic_0	0.9802±0.0000	0.7068	0.7040
sipu_d31_0	0.6001±0.0085	0.1846	0.1787
sipu_a1_0	0.7499±0.0000	0.3269	0.2229
sipu_r15_0	0.9258±0.0000	0.4551	0.2552
sipu_a2_0	0.7555±0.0000	0.1685	0.1685
sipu_a3_0	0.7434±0.0000	0.1410	0.1410
sipu_s1_0	0.9888±0.0000	0.3695	0.2581
sipu_s2_0	0.9405±0.0000	0.2581	0.2579

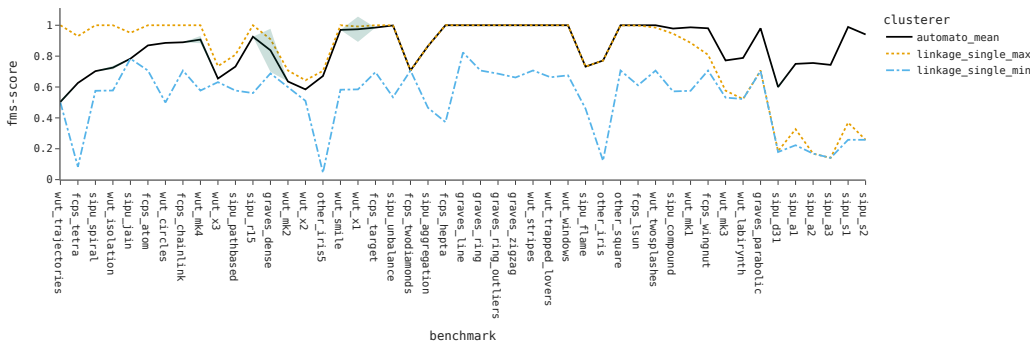


Figure 9: Comparison of AuToMATo and agglomerative clustering with single linkage.

Table 6: Fowlkes-Mallows scores of AuToMATo vs. TTK clustering algorithm

Dataset	automato_mean	automato_std	ttk
wut_trajectories_0	0.5038±0.0107	0.0107	0.8682
fcps_tetra_0	0.6261±0.0000	0.0000	0.9043
wut_x3_0	0.5153±0.0000	0.0000	0.7818
wut_isolation_0	0.7256±0.0113	0.0113	0.9416
sipu_a1_0	0.7499±0.0000	0.0000	0.9143
wut_x2_0	0.5846±0.0000	0.0000	0.7283
sipu_flame_0	0.7320±0.0000	0.0000	0.8562
sipu_aggregation_0	0.8652±0.0000	0.0000	0.9692
graves_zigzag_1	0.6720±0.0000	0.0000	0.7698
other_iris_0	0.7715±0.0000	0.0000	0.8639
sipu_jain_0	0.7837±0.0000	0.0000	0.8182

Continued on next page

1026
1027
1028
1029
1030
1031
1032
1033
1034
1035
1036
1037
1038
1039
1040
1041
1042
1043
1044
1045
1046
1047
1048
1049
1050
1051
1052
1053
1054
1055
1056
1057
1058
1059
1060
1061
1062
1063
1064
1065
1066
1067
1068
1069
1070
1071
1072
1073
1074
1075
1076
1077
1078
1079

Table 6: Fowlkes-Mallows scores of AuToMATo vs. TTK clustering algorithm

Dataset	automato_mean	automato_std	ttk
graves_dense_0	0.8377±0.1396	0.1396	0.8615
sipu_r15_0	0.9258±0.0000	0.0000	0.9374
wut_mk3_0	0.7720±0.0000	0.0000	0.7755
wut_labirynth_0	0.7884±0.0000	0.0000	0.7884
fcps_chainlink_0	0.8896±0.0000	0.0000	0.8896
wut_smile_0	0.9681±0.0000	0.0000	0.9681
wut_stripes_0	1.0000±0.0000	0.0000	1.0000
graves_ring_outliers_0	1.0000±0.0000	0.0000	1.0000
wut_smile_1	0.9701±0.0000	0.0000	0.9701
sipu_unbalance_0	0.9986±0.0008	0.0008	0.9951
sipu_s1_0	0.9888±0.0000	0.0000	0.9843
sipu_s2_0	0.9405±0.0000	0.0000	0.9311
other_iris5_0	0.6712±0.0000	0.0000	0.6612
fcps_atom_0	0.8694±0.0000	0.0000	0.8472
wut_x3_1	0.6546±0.0000	0.0000	0.6312
sipu_d31_0	0.6001±0.0085	0.0085	0.5667
fcps_hepta_0	1.0000±0.0000	0.0000	0.9594
graves_parabolic_1	0.6916±0.0000	0.0000	0.6473
sipu_r15_2	0.4867±0.0000	0.0000	0.4322
sipu_pathbased_0	0.6517±0.0000	0.0000	0.5947
sipu_spiral_0	0.7028±0.0000	0.0000	0.6422
sipu_r15_1	0.5436±0.0000	0.0000	0.4827
sipu_pathbased_1	0.7322±0.0000	0.0000	0.6668
fcps_target_0	0.9850±0.0000	0.0000	0.9185
wut_x1_0	0.9741±0.0818	0.0818	0.8960
wut_twosplashes_0	1.0000±0.0000	0.0000	0.9140
wut_mk4_0	0.9072±0.0234	0.0234	0.8050
wut_mk2_0	0.6356±0.0000	0.0000	0.5302
graves_parabolic_0	0.9802±0.0000	0.0000	0.8653
sipu_compound_4	0.9442±0.0000	0.0000	0.8145
fcps_wingnut_0	0.9805±0.0000	0.0000	0.8497
wut_circles_0	0.8857±0.0000	0.0000	0.7543
wut_mk1_0	0.9866±0.0000	0.0000	0.8148
fcps_twodiamonds_0	0.7067±0.0000	0.0000	0.5251
sipu_compound_0	0.8616±0.0000	0.0000	0.6728
sipu_compound_1	0.9786±0.0000	0.0000	0.7892
graves_line_0	1.0000±0.0000	0.0000	0.7917
fcps_lsun_0	1.0000±0.0000	0.0000	0.7897
wut_trapped_lovers_0	1.0000±0.0000	0.0000	0.7859
other_square_0	1.0000±0.0000	0.0000	0.7774
graves_zigzag_0	1.0000±0.0000	0.0000	0.7686
graves_ring_0	1.0000±0.0000	0.0000	0.7278
sipu_a2_0	0.7555±0.0000	0.0000	0.4641
wut_windows_0	1.0000±0.0000	0.0000	0.5853
sipu_a3_0	0.7434±0.0000	0.0000	0.1882

Table 7: Fowlkes-Mallows scores of AuToMATo vs. hierarchical clustering with complete linkage

Dataset	automato_mean	linkage_complete_max	linkage_complete_min
sipu_r15_2	0.4867±0.0000	1.0000	0.2256
wut_trajectories_0	0.5038±0.0107	1.0000	0.1706
sipu_r15_1	0.5436±0.0000	0.8954	0.2516
wut_x3_1	0.6546±0.0000	0.9740	0.2004

Continued on next page

1080
1081
1082
1083
1084
1085
1086
1087
1088
1089
1090
1091
1092
1093
1094
1095
1096
1097
1098
1099
1100
1101
1102
1103
1104
1105
1106
1107
1108
1109
1110
1111
1112
1113
1114
1115
1116
1117
1118
1119
1120
1121
1122
1123
1124
1125
1126
1127
1128
1129
1130
1131
1132
1133

Table 7: Fowlkes-Mallows scores of AuToMATo vs. hierarchical clustering with complete linkage

Dataset	automato_mean	linkage_complete_max	linkage_complete_min
fcps_tetra_0	0.6261±0.0000	0.9356	0.0651
sipu_d31_0	0.6001±0.0085	0.8733	0.2717
wut_x3_0	0.5153±0.0000	0.7842	0.2477
sipu_a3_0	0.7434±0.0000	0.8979	0.2294
wut_mk3_0	0.7720±0.0000	0.9207	0.0711
wut_x2_0	0.5846±0.0000	0.7298	0.1964
sipu_a2_0	0.7555±0.0000	0.8992	0.2642
sipu_jain_0	0.7837±0.0000	0.9116	0.1288
wut_circles_0	0.8857±0.0000	1.0000	0.1761
sipu_r15_0	0.9258±0.0000	0.9799	0.3372
sipu_a1_0	0.7499±0.0000	0.8040	0.3092
graves_zigzag_1	0.6720±0.0000	0.7119	0.3039
sipu_aggregation_0	0.8652±0.0000	0.9030	0.1246
other_iris_0	0.7715±0.0000	0.8064	0.0680
wut_x1_0	0.9741±0.0818	1.0000	0.2326
sipu_unbalance_0	0.9986±0.0008	0.9988	0.5774
fcps_hepta_0	1.0000±0.0000	1.0000	0.4321
fcps_twodiamonds_0	0.7067±0.0000	0.7060	0.0916
sipu_flame_0	0.7320±0.0000	0.7276	0.0834
sipu_compound_0	0.8616±0.0000	0.8472	0.1567
sipu_s1_0	0.9888±0.0000	0.9563	0.3672
sipu_pathbased_0	0.6517±0.0000	0.6022	0.1384
sipu_pathbased_1	0.7322±0.0000	0.6709	0.1539
graves_parabolic_1	0.6916±0.0000	0.6168	0.1482
sipu_compound_1	0.9786±0.0000	0.9023	0.1366
sipu_compound_4	0.9442±0.0000	0.8652	0.1408
graves_dense_0	0.8377±0.1396	0.7584	0.3538
wut_mk1_0	0.9866±0.0000	0.8950	0.1591
wut_smile_1	0.9701±0.0000	0.8697	0.3562
graves_parabolic_0	0.9802±0.0000	0.8610	0.1088
wut_mk2_0	0.6356±0.0000	0.5032	0.1096
other_iris5_0	0.6712±0.0000	0.5305	0.0451
fcps_atom_0	0.8694±0.0000	0.7278	0.1364
wut_smile_0	0.9681±0.0000	0.8206	0.3793
sipu_s2_0	0.9405±0.0000	0.7642	0.3114
wut_mk4_0	0.9072±0.0234	0.7282	0.1297
fcps_target_0	0.9850±0.0000	0.7881	0.1934
fcps_lsun_0	1.0000±0.0000	0.7668	0.1377
fcps_wingnut_0	0.9805±0.0000	0.7406	0.0816
graves_ring_0	1.0000±0.0000	0.7589	0.1849
graves_ring_outliers_0	1.0000±0.0000	0.7528	0.1995
wut_labirynth_0	0.7884±0.0000	0.4893	0.1426
fcps_chainlink_0	0.8896±0.0000	0.5889	0.0919
sipu_spiral_0	0.7028±0.0000	0.3512	0.1424
wut_isolation_0	0.7256±0.0113	0.3397	0.1153
graves_line_0	1.0000±0.0000	0.5972	0.1909
other_square_0	1.0000±0.0000	0.5846	0.1142
graves_zigzag_0	1.0000±0.0000	0.5505	0.2042
wut_twosplashes_0	1.0000±0.0000	0.5310	0.2771
wut_stripes_0	1.0000±0.0000	0.5136	0.0706
wut_trapped_lovers_0	1.0000±0.0000	0.4790	0.0579
wut_windows_0	1.0000±0.0000	0.4349	0.0781

1134
1135
1136
1137
1138
1139
1140
1141
1142
1143
1144
1145
1146
1147
1148
1149
1150
1151
1152
1153
1154
1155
1156
1157
1158
1159
1160
1161
1162
1163
1164
1165
1166
1167
1168
1169
1170
1171
1172
1173
1174
1175
1176
1177
1178
1179
1180
1181
1182
1183
1184
1185
1186
1187

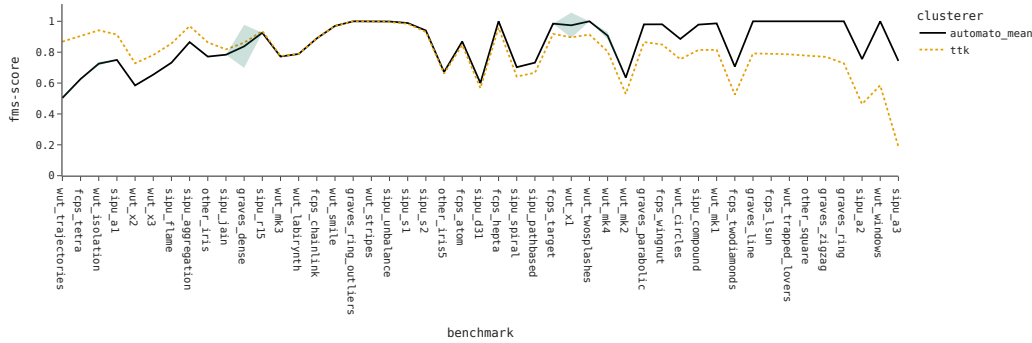


Figure 10: Comparison of AuToMATo and the TTK-algorithm.

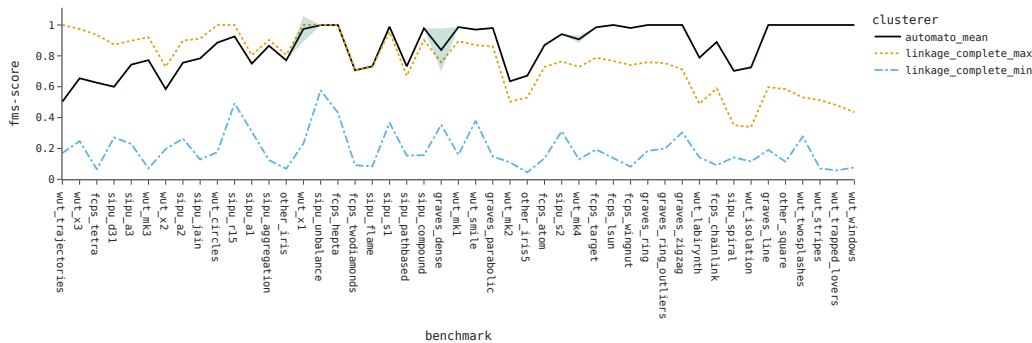


Figure 11: Comparison of AuToMATo and agglomerative clustering with complete linkage.

Table 8: Fowlkes-Mallows scores of AuToMATo vs. hierarchical clustering with Ward linkage

Dataset	automato_mean	linkage_ward_max	linkage_ward_min
wut_x3_0	0.5153±0.0000	0.8537	0.2203
sipu_d31_0	0.6001±0.0085	0.9223	0.2766
sipu_a3_0	0.7434±0.0000	0.9377	0.2889
sipu_a2_0	0.7555±0.0000	0.9360	0.2653
sipu_a1_0	0.7499±0.0000	0.9166	0.2464
wut_x2_0	0.5846±0.0000	0.7219	0.2076
sipu_r15_2	0.4867±0.0000	0.5893	0.1868
graves_zigzag_1	0.6720±0.0000	0.7358	0.2693
sipu_r15_0	0.9258±0.0000	0.9832	0.4072
sipu_r15_1	0.5436±0.0000	0.5993	0.2082
wut_x3_1	0.6546±0.0000	0.7090	0.1795
wut_x1_0	0.9741±0.0818	1.0000	0.2429
sipu_unbalance_0	0.9986±0.0008	1.0000	0.2063
fcps_hepta_0	1.0000±0.0000	1.0000	0.4314
sipu_s1_0	0.9888±0.0000	0.9844	0.2453
sipu_pathbased_0	0.6517±0.0000	0.6251	0.1370
sipu_s2_0	0.9405±0.0000	0.9085	0.2177
sipu_pathbased_1	0.7322±0.0000	0.6844	0.1523
fcps_tetra_0	0.6261±0.0000	0.5622	0.0651

Continued on next page

1188
1189
1190
1191
1192
1193
1194
1195
1196
1197
1198
1199
1200
1201
1202
1203
1204
1205
1206
1207
1208
1209
1210
1211
1212
1213
1214
1215
1216
1217
1218
1219
1220
1221
1222
1223
1224
1225
1226
1227
1228
1229
1230
1231
1232
1233
1234
1235
1236
1237
1238
1239
1240
1241

Table 8: Fowlkes-Mallows scores of AuToMATo vs. hierarchical clustering with Ward linkage

Dataset	automato_mean	linkage_ward_max	linkage_ward_min
graves_dense_0	0.8377±0.1396	0.7454	0.2684
wut_trajectories_0	0.5038±0.0107	0.3933	0.0981
other_iris_0	0.7715±0.0000	0.6377	0.0680
fcps_atom_0	0.8694±0.0000	0.7272	0.1016
graves_parabolic_1	0.6916±0.0000	0.5260	0.1301
fcps_target_0	0.9850±0.0000	0.7759	0.1503
other_iris5_0	0.6712±0.0000	0.4508	0.0451
sipu_aggregation_0	0.8652±0.0000	0.6064	0.1215
sipu_flame_0	0.7320±0.0000	0.4555	0.0819
sipu_compound_0	0.8616±0.0000	0.5846	0.1523
wut_mk3_0	0.7720±0.0000	0.4911	0.0711
fcps_twodiamonds_0	0.7067±0.0000	0.3967	0.0861
sipu_jain_0	0.7837±0.0000	0.4668	0.1201
wut_mk1_0	0.9866±0.0000	0.6564	0.1473
fcps_lsun_0	1.0000±0.0000	0.6659	0.1270
sipu_compound_4	0.9442±0.0000	0.5793	0.1368
sipu_spiral_0	0.7028±0.0000	0.3100	0.1384
wut_labyrinth_0	0.7884±0.0000	0.3749	0.0961
sipu_compound_1	0.9786±0.0000	0.5648	0.1327
wut_twosplashes_0	1.0000±0.0000	0.5817	0.2046
wut_smile_1	0.9701±0.0000	0.5246	0.2352
wut_smile_0	0.9681±0.0000	0.5179	0.2505
wut_mk2_0	0.6356±0.0000	0.1814	0.0997
graves_zigzag_0	1.0000±0.0000	0.5448	0.1809
wut_isolation_0	0.7256±0.0113	0.2309	0.0800
graves_line_0	1.0000±0.0000	0.5045	0.1667
wut_circles_0	0.8857±0.0000	0.3681	0.1323
fcps_chainlink_0	0.8896±0.0000	0.3407	0.0894
wut_mk4_0	0.9072±0.0234	0.3557	0.1079
graves_parabolic_0	0.9802±0.0000	0.4184	0.0935
graves_ring_0	1.0000±0.0000	0.4135	0.1427
graves_ring_outliers_0	1.0000±0.0000	0.4082	0.1515
fcps_wingnut_0	0.9805±0.0000	0.3229	0.0727
other_square_0	1.0000±0.0000	0.3347	0.1007
wut_windows_0	1.0000±0.0000	0.2833	0.0663
wut_trapped_lovers_0	1.0000±0.0000	0.2552	0.0471
wut_stripes_0	1.0000±0.0000	0.1922	0.0552

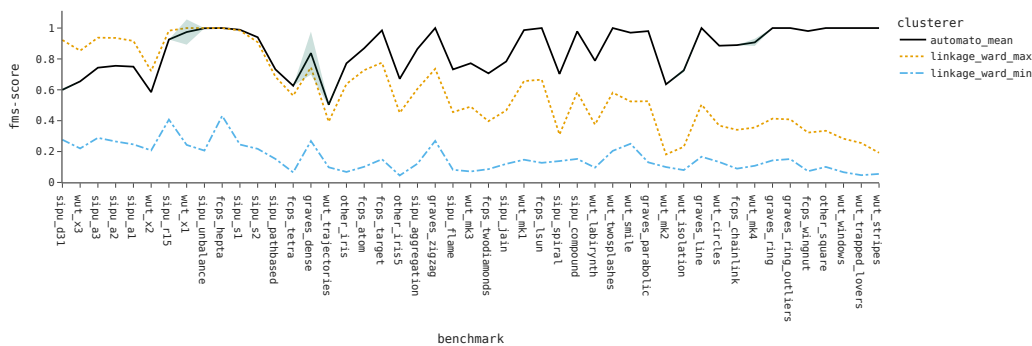


Figure 12: Comparison of AuToMATo and agglomerative clustering with Ward linkage.

1242
1243
1244
1245
1246
1247
1248
1249
1250
1251
1252
1253
1254
1255
1256
1257
1258
1259
1260
1261
1262
1263
1264
1265
1266
1267
1268
1269
1270
1271
1272
1273
1274
1275
1276
1277
1278
1279
1280
1281
1282
1283
1284
1285
1286
1287
1288
1289
1290
1291
1292
1293
1294
1295

Table 9: Fowlkes-Mallows scores of AuToMATo vs. FINCH

Dataset	automato_mean	automato_std	finch
wut_x3_0	0.5153±0.0000	0.0000	0.7970
sipu_d31_0	0.6001±0.0085	0.0085	0.8657
sipu_a3_0	0.7434±0.0000	0.0000	0.8306
wut_x2_0	0.5846±0.0000	0.0000	0.6671
wut_mk3_0	0.7720±0.0000	0.0000	0.8503
other_iris5_0	0.6712±0.0000	0.0000	0.7008
sipu_a2_0	0.7555±0.0000	0.0000	0.7635
wut_x3_1	0.6546±0.0000	0.0000	0.6619
sipu_unbalance_0	0.9986±0.0008	0.0008	0.9998
sipu_r15_0	0.9258±0.0000	0.0000	0.9083
wut_mk1_0	0.9866±0.0000	0.0000	0.9655
other_iris_0	0.7715±0.0000	0.0000	0.7477
sipu_a1_0	0.7499±0.0000	0.0000	0.7124
sipu_r15_2	0.4867±0.0000	0.0000	0.4156
graves_zigzag_1	0.6720±0.0000	0.0000	0.5965
graves_dense_0	0.8377±0.1396	0.1396	0.7615
sipu_r15_1	0.5436±0.0000	0.0000	0.4641
sipu_s1_0	0.9888±0.0000	0.0000	0.8728
fcps_hepta_0	1.0000±0.0000	0.0000	0.8794
fcps_atom_0	0.8694±0.0000	0.0000	0.7319
fcps_tetra_0	0.6261±0.0000	0.0000	0.4680
sipu_s2_0	0.9405±0.0000	0.0000	0.7282
wut_x1_0	0.9741±0.0818	0.0818	0.7607
graves_parabolic_1	0.6916±0.0000	0.0000	0.4446
sipu_flame_0	0.7320±0.0000	0.0000	0.4767
sipu_pathbased_0	0.6517±0.0000	0.0000	0.3440
sipu_compound_0	0.8616±0.0000	0.0000	0.5390
sipu_pathbased_1	0.7322±0.0000	0.0000	0.3828
wut_trajectories_0	0.5038±0.0107	0.0107	0.1503
fcps_lsun_0	1.0000±0.0000	0.0000	0.6206
sipu_compound_4	0.9442±0.0000	0.0000	0.5493
sipu_jain_0	0.7837±0.0000	0.0000	0.3824
sipu_compound_1	0.9786±0.0000	0.0000	0.5356
sipu_spiral_0	0.7028±0.0000	0.0000	0.2553
wut_mk4_0	0.9072±0.0234	0.0234	0.4331
wut_mk2_0	0.6356±0.0000	0.0000	0.1478
sipu_aggregation_0	0.8652±0.0000	0.0000	0.3674
fcps_twodiamonds_0	0.7067±0.0000	0.0000	0.1837
wut_smile_0	0.9681±0.0000	0.0000	0.4452
wut_smile_1	0.9701±0.0000	0.0000	0.4181
fcps_target_0	0.9850±0.0000	0.0000	0.4297
wut_labirynth_0	0.7884±0.0000	0.0000	0.2209
wut_isolation_0	0.7256±0.0113	0.0113	0.1440
wut_twosplashes_0	1.0000±0.0000	0.0000	0.4162
graves_zigzag_0	1.0000±0.0000	0.0000	0.4094
graves_parabolic_0	0.9802±0.0000	0.0000	0.3343
graves_line_0	1.0000±0.0000	0.0000	0.3379
fcps_chainlink_0	0.8896±0.0000	0.0000	0.2224
fcps_wingnut_0	0.9805±0.0000	0.0000	0.3110
graves_ring_0	1.0000±0.0000	0.0000	0.2770
wut_trapped_lovers_0	1.0000±0.0000	0.0000	0.2767
other_square_0	1.0000±0.0000	0.0000	0.2393
graves_ring_outliers_0	1.0000±0.0000	0.0000	0.2248

Continued on next page

1296
1297
1298
1299
1300
1301
1302
1303
1304
1305
1306
1307
1308
1309
1310
1311
1312
1313
1314
1315
1316
1317
1318
1319
1320
1321
1322
1323
1324
1325
1326
1327
1328
1329
1330
1331
1332
1333
1334
1335
1336
1337
1338
1339
1340
1341
1342
1343
1344
1345
1346
1347
1348
1349

Table 9: Fowlkes-Mallows scores of AuToMATo vs. FINCH

Dataset	automato_mean	automato_std	finch
wut_circles_0	0.8857±0.0000	0.0000	0.0976
wut_windows_0	1.0000±0.0000	0.0000	0.1166
wut_stripes_0	1.0000±0.0000	0.0000	0.0867

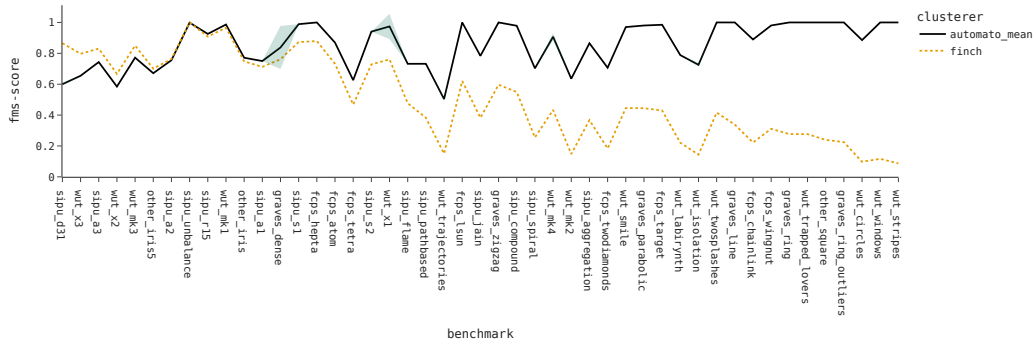


Figure 13: Comparison of AuToMATo and FINCH.